Available online at www.sciencedirect.com

SCIENCE DIRECT®

Thermochimica Acta 419 (2004) 119–129

thermochimica acta

www.elsevier.com/locate/tca

Thermal decomposition of metazeunerite—a high-resolution thermogravimetric and hot-stage Raman spectroscopic study

Ray L. Frost*, Matt L. Weier, Moses O. Adebajo

Inorganic Materials Research Program, School of Physical and Chemical Sciences, Queensland University of Technology,
G.P.O. Box 2434, Brisbane, Qld 4001, Australia

Received 7 September 2003; received in revised form 16 February 2004; accepted 18 February 2004

Abstract

A combination of high-resolution thermogravimetric analysis coupled to a gas evolution mass spectrometer has been used to study the thermal decomposition of metazeunerite $\{Cu(H_2O)_4\}(H_2O)_4[(UO_2)(AsO_4)]_2$. Five stages of weight loss are observed at 48, 88, 125, 882 and 913 °C. In the first three stages 2, 4 and 2 mol of water are lost. In stages 4 and 5, some As_2O_5 units are lost and it is probable that reduction of the anhydrous phase $Cu[(UO_2)(AsO_4)]_2$ occurs. The stages of dehydration were confirmed by the use of evolved water vapour mass spectroscopy. Changes in the structure of metazeunerite were followed by the use of Raman microscopy in conjunction with a thermal stage. Two Raman bands are observed at 818 and 811 cm^{-1} and are assigned to the ν_1 symmetric stretching modes of the UO_2 units. The UO_2 Raman antisymmetric stretching mode was observed at 890 cm^{-1}. No AsO_4 stretching vibrations were observed until after two stages of dehydration of the metazeunerite. The AsO_4 ν_4 bending modes show complexity with bands observed at 463, 446, 396 and 380 cm^{-1}. Thermal treatment results in the removal of this degeneracy. The ν_2 band of the AsO_4 units is observed at 320 cm^{-1}. Raman bands at 275 and 235 cm^{-1} are attributed to the ν_2 bending modes of the $(UO_2)^{2+}$ units. The use of the hot-stage Raman microscope enables low-temperature phase changes brought about through dehydration to be studied.

Keywords: Autunite; Meta-autunites; Metazeunerite; Dehydration; Dehydroxylation; Raman spectroscopy; High-resolution thermogravimetric analysis

1. Introduction

There are more than 200 uranium minerals, many of which exist in Australian deposits [1]. The chemistry of uranium is important for the solution of environmental problems; for example the remediation of contaminated sites and the restoration of soils such as might be found at Woomera, Australia [2,3]. Uranyl phosphates and arsenates form one of the largest and most widespread group of uranium minerals [4]. The minerals are known as autunites and also as the uranyl micas. Many of these minerals may be found in quite widespread parts of Australia [5]. The autunite group of minerals are uranyl arsenates and phosphates with symmetries ranging from tetragonal to triclinic. The minerals have a general formula $M(UO_2)_2(XO_4)_2\cdot8–12H_2O$, where M may be Ba, Ca, Cu, Fe^{2+}, Mg, Mn^{2+} or 1/2(HAl) and X is As or P. Autunites are common minerals, yet have been rarely studied in terms of thermal analysis [6–9] and certainly not in terms of Raman spectroscopy. The minerals have a layer-like structure [8,10,11]. The cations and water are located in the interlayer space. The mineral autunite has the formula $Ca[(UO_2)_2(PO_4)]_2\cdot11H_2O$. The structure of a synthetic autunite has been solved [10]. Autunite is orthorhombic [10] and saléeite is monoclinic [12,13]. The structure contains the well-known autunite-type sheet with composition $[(UO_2)(PO_4)]$, resulting from the sharing of equatorial vertices of the uranyl square bipyramids with the phosphate or arsenate tetrahedra [14]. The calcium atom in the interlayer is coordinated by seven H_2O groups and two longer distances to uranyl apical O atoms. Two independent H_2O groups are held in the structure only by hydrogen bonding [10].

Most uranyl minerals are hydrated and as such water plays a significant role in their structures. It is common for water to play a major role in the degree of polymerisation because of the asymmetric nature of hydrogen bonding systems. Water may bond to the interstitial cation or may simply be held in

---

* Corresponding author. Tel.: +61-7-3864-2407;
fax: +61-7-3864-1804.
E-mail address: r.frost@qut.edu.au (R.L. Frost).

0040-6031/$ – see front matter © 2004 Elsevier B.V. All rights reserved.
doi:10.1016/j.tca.2004.02.006

the structure through hydrogen bonding. Water groups play an important role in satisfying bond-valence requirements. The role of water and the number of water units in the empirical formula determines structural arrangements in the uranyl mica interlayer [4]. For example:

$$\mathrm{Ca(UO_2)_2(PO_4)_2 \cdot 11H_2O} \text{ (autunite)} \rightarrow \mathrm{Ca(UO_2)_2(PO_4)_2 \cdot 8H_2O} \text{ (meta-autunite)}$$

$$\mathrm{Ca(UO_2)_2(PO_4)_2 \cdot 8H_2O} \text{ (meta-autunite)} \rightarrow \mathrm{Ca(UO_2)_2(PO_4)_2 \cdot \mathit{x}H_2O} \text{ (partially dehydrated meta-autunite).}$$

Burns et al. [15] proposed that uranyl mineral structures be based upon a topological arrangement of anions within each sheet as a convenient basis for the classification of these sheets [15]. The difference between the autunite group and meta-autunite is simply the number of water molecules in the formula. One major difference between the autunite and meta-autunite groups is their water content. The moles of water in different autunite species may differ and as a group range from 10 to 12 mol. On the other hand, the moles of water in the meta-autunite group ranges from 6 to 8 mol. The structure and hydration state of meta-autunite have not been satisfactorily determined. Zeunerite is the mineral $\{Cu(H_2O)_4\}(H_2O)_8[(UO_2)(AsO_4)]_2$ and metazeunerite is the mineral $\{Cu(H_2O)_4\}(H_2O)_4[(UO_2)(AsO_4)]_2$ [16,17].

The use of infrared spectroscopy to study the chemical reactions as illustrated in the above thermal stages of dehydration is difficult in the lower temperature ranges. However, Raman spectroscopy combined with a hot stage lends itself as the technique of choice for studying the chemical reactions during dehydration. The structures of copper-based synthetic autunites, namely torbernite, metatorbernite, zeunerite and metazeunerite have been solved [16]. Zeunerite and metazeunerite are isostructural with torbernite and metatorbernite [16]. These minerals contain the autunite-type sheet, of composition $[(UO_2)(AsO_4)]^-$ or $[(UO_2)(PO_4)]^-$, which involves the sharing of equatorial vertices of uranyl square bipyramids with phosphate (or arsenate) tetrahedra. According to Locock and Burns [16], there is a symmetrically independent H_2O group held in each structure by hydrogen bonding, which in zeunerite forms square planar sets of interstitial water groups both above and below the planes of the Cu^{2+} atoms. In the metazeunerite structure, the sets of interstitial water are either above or below the planes of the Cu^{2+} cations. Upon dehydration of the zeunerite to metazeunerite, not only is there a loss of 4 mol of water but the space groups change and the orientations of the uranyl arsenate sheets change. Our interest in minerals with clay-like structures causes our motivation in this research as does the search for fundamental knowledge of minerals containing copper and arsenate anions [2,3,18,19]. In this work, we report the thermal transformation of metazeunerite, a copper-based uranyl arsenate using a combination of high-resolution thermogravimetry coupled to an evolved gas mass spectrometer and hot-stage Raman microscopy.

2. Experimental

2.1. Minerals

Metazeunerite (M20948), was obtained from Museum Victoria and originated from Gilgai, New England, NSW. The mineral was analysed by X-ray diffraction for phase purity and by electron probe using energy dispersive techniques for quantitative chemical composition.

2.2. X-ray diffraction

X-ray diffraction patterns were collected using a Philips X'pert wide angle X-ray diffractometer, operating in step scan mode, with Cu Kα radiation (1.54052 Å). Patterns were collected in the range 3–90° 2θ with a step size of 0.02° and a rate of 30 s per step. Samples were prepared as a randomly orientated powder on a petroleum jelly coated glass slide. Data collection and evaluation were performed with PC-APD 3.6 software. Profile fitting was applied to extract information on the microstructure and structural defects of metazeunerite and its alteration products. The profile fitting option of the software uses a model that employs 12 intrinsic parameters to describe the profile, the instrumental aberration and wavelength dependent contributions to the profile.

2.3. Thermal analysis

Thermal decomposition of the metazeunerite was carried out in a TA® Instruments incorporated high-resolution thermogravimetric analyser (series Q500) in a flowing nitrogen atmosphere (80 cm^3/min). Approximately 50 mg of sample was heated in an open platinum crucible at a rate of 2.0 °C/min up to 500 °C. With the quasi-isothermal, quasi-isobaric heating programme of the instrument the furnace temperature was regulated precisely to provide a uniform rate of decomposition in the main decomposition stage. The TGA instrument was coupled to a Balzers (Pfeiffer) mass spectrometer for gas analysis. Only water vapour, carbon dioxide and oxygen were analysed.

2.4. Hot-stage Raman microprobe spectroscopy

The crystals of metazeunerite were placed and oriented on the stage of an Olympus BHSM microscope, equipped with 10× and 50× objectives and part of a Renishaw 1000 Raman microscope system, which also includes a monochromator, a filter system and a charge coupled device (CCD). Raman spectra were excited by a HeNe laser (633 nm) at a resolution of 2 cm^{-1} in the range between 100 and 4000 cm^{-1}. Repeated acquisition using the highest magnification was accumulated to improve the signal to noise ratio. Spectra were calibrated using the 520.5 cm^{-1} line of a silicon wafer. In order to ensure that the correct spectra are obtained, the incident excitation radiation was scrambled. Previous studies by the authors provide more details of the experimental technique [3,20–22]. Spectra at elevated temperatures were obtained using a Linkam thermal stage (Scientific Instruments Ltd., Waterfield, Surrey, England). Details of the technique have been published by the authors [2,18,19,23–25]. Spectral manipulation such as baseline adjustment, smoothing and normalisation was performed using the GRAMS® software package (Galactic Industries Corporation, Salem, NH, USA).

3. Results and discussion

3.1. X-ray diffraction of metazeunerite

The analysis of the sample labelled as metazeunerite (M20948) from Museum Victoria is shown in Table 1 and compared with the XRD data obtained from JCPDS data base. A study of the data in the table appears to show that the mineral is a mixture of zeunerite and metazeunerite. The *d*(0 0 1) spacing of 10.35 Å for the mineral used in this research corresponds with the 10.3 Å of zeunerite. The *d* spacing of 8.68 Å corresponds to that of 8.63 Å for metazeunerite.

3.2. High-resolution thermogravimetric analysis and mass spectrometric analysis

The high-resolution thermogravimetric analysis of metazeunerite is shown in Fig. 1a and b. Four steps are involved with the loss of water and two with the loss or reduction of arsenate anions. The first step occurs at 48 °C, the second at 88 °C, the third at 138 °C and the last step involving water at 255 °C. This last step appears as a broad continuum over an extended temperature range from around 150 to 250 °C. The weight loss steps are 3.45, 7.05, 0.87 and 3.46%, respectively. The total weight loss is 14.83%. The theoretical weight loss for $Cu(UO_2)_2(AsO_4)_2{\cdot}8H_2O$ is 14.05%. The difference between the experimental and theoretical mass losses may be accounted for by adsorbed water. Whilst no low-temperature (<40 °C) mass loss is observed in the HRTG experiment, a low-temperature water vapour evolution is observed in the MS pattern. This may be attributed to the loss of adsorbed water. This means that the number of moles of water lost in the first step is 2, in the second step 4 and in the third and fourth steps 2. The loss of arsenate occurs over two steps at 882 and 913 °C (Fig. 1b). The mass loss steps are 8.3 and 4.1%. The theoretical weight loss for arsenate is 27.0%. This means that about 50% of the AsO_4 units are lost at 882 and 913 °C. The upper temperature limits of the HRTG are 1000 °C and it is thought that the remainder of the AsO_4 units may be accounted for by reduction of the U, As and even Cu at the higher temperatures. The mass spectrum of water is shown in Fig. 2. This figure shows the MS = 18 curve and the DTG curve. The two curves have the same patterns precisely. The figure shows that evolved water vapour mass as the metazeunerite is thermally decomposed. The temperatures of the mass gain are 47, 88.6, 136 and 257 °C. These temperatures match the temperatures of the mass loss steps with absolute precision. The MS of water shows an additional evolved mass gain at 28.7 °C which was not observed in the HRTG patterns and is ascribed to adsorbed water.

3.2.1. Stages of the thermal decomposition of metazeunerite

Metazeunerite may be written as $\{Cu(H_2O)_4\}(H_2O)_4[(UO_2)(AsO_4)]_2$ [16]. The units in the square bracket represent the uranyl arsenate sheet and the remaining part of the formula the interlayer contents. Writing the formula of metazeunerite as such shows the hydration of the Cu^{2+} and the additional water molecules held in place in the interlayer by hydrogen bonding. In the structure of metazeunerite, the Cu^{2+} is coordinated by four water molecules and by two longer bonds to the apical oxygen atoms of the uranyl ions. Uranyl micas are layered structures with water playing a dominant role in their structures. In this case, the hydrated cations fit between the uranyl arsenate layers [17]. In the case of metazeunerite, the uranyl arsenate surface may be considered to be multiple units of $(UO_2{\cdot}AsO_4)_n$ and functions like a polymeric anion. The anion is counterbalanced by the hydrated copper(II) cation in the interlayer. Dehydration of metazeunerite results in the loss of water firstly from the interlayer and secondly from around the copper(II) ion.

The mechanism for the dehydration of metazeunerite is as follows:

- *Stage 1*: $\{Cu(H_2O)_4\}(H_2O)_4[(UO_2)(AsO_4)]_2 \rightarrow \{Cu(H_2O)_4\}(H_2O)_2[(UO_2)(AsO_4)]_2 + 2H_2O$ (48 °C)
- *Stage 2*: $\{Cu(H_2O)_4\}(H_2O)_2[(UO_2)(AsO_4)]_2 \rightarrow \{Cu(H_2O)_2\}[(UO_2)(AsO_4)]_2 + 4H_2O$ (88 °C)
- *Stage 3*: $\{Cu(H_2O)_2\}[(UO_2)(AsO_4)]_2 \rightarrow Cu[(UO_2)(AsO_4)]_2 + 2H_2O$ (125–250 °C)
- *Stages 4 and 5*: $Cu(UO_2)_2(AsO_4)_2 \rightarrow CuO(UO_2)_2(AsO_4) + 0.5As_2O_5$ (882 and 913 °C)

The thermal decomposition of metazeunerite may be considered as occurring in a sequence of stages. In stage 1 at 48 °C, 2 mol of water are lost. In stage 2, 4 mol of water are lost and in stage 3 a further 2 mol of water are lost. Thus, in three successive stages all 8 mol of water are lost resulting in an anhydrous compound $(Cu(UO_2)_2(AsO_4)_2)$. It is not known whether this chemical retains its layered structure or forms a three-dimensional structure with Cu linking the uranyl arsenate groups. The two higher temperature stages are attributed to the loss of arsenate as As_2O_5. In these steps, it is not certain whether all the As is lost or that some is retained to higher temperatures in some reduced form. The upper temperature limit of the HRTG is 1000 °C and any weight losses above this temperature are not determined. It is probable that not all the arsenate is lost at 882 and 913 °C even though the experimental weight

Table 1
X-ray diffraction data analysis of metazeunerite

Sample			00-017-0150 zeunerite				00-017-0146 metazeunerite			
d (Å)	2θ (°)	I (%)	d (Å)	2θ (°)	I (%)	$h\,k\,l$	d (Å)	2θ (°)	I (%)	$h\,k\,l$
10.35981	8.5353	100	10.3	8.578	100	0 0 2	8.86	9.975	100	0 0 2
8.68233	10.1884	86	6.81	12.99	30	1 0 1	6.63	13.344	5	1 0 1
6.76185	13.0934	2	5.2	17.038	70	0 0 4	5.57	15.898	80	1 0 2
5.49692	16.1245	1	4.98	17.796	50	1 0 3	5.1	17.374	60	1 1 0
5.19651	17.0634	38	4.58	19.365	5	1 1 2	4.38	20.258	30	0 0 4
5.05522	17.544	1	3.59	24.78	100	2 0 0	3.73	23.836	100	1 0 4
4.98093	17.8078	2	3.39	26.268	50	2 0 2	3.57	24.921	70	2 0 0
4.35188	20.4076	10	3.16	28.218	10	2 1 1	3.3	26.998	80	1 1 4
3.71212	23.973	6	3.06	29.16	5	2 1 2	3.13	28.494	5	1 0 5
3.60126	24.7224	8	2.95	30.273	30	2 0 4	2.98	29.961	40	2 1 2
3.55205	25.0705	2	2.91	30.699	5	2 1 3	2.77	32.292	10	2 1 3
3.46969	25.6756	1	2.86	31.249	10	1 1 6	2.69	33.28	20	1 0 6
3.3883	26.3033	3	2.74	32.655	30	1 0 7	2.57	34.882	40	2 1 4
3.29142	27.092	1	2.53	35.452	40	2 2 0	2.51	35.744	40	2 2 0
2.95158	30.282	1	2.46	36.496	30	2 2 2	2.41	37.281	30	2 2 2
2.74586	32.5838	2	2.37	37.934	5	3 0 1	2.29	39.312	10	3 0 2
2.69008	33.3073	1	2.32	38.784	20	1 1 8	2.24	40.227	20	3 1 0
2.60112	34.452	1	2.26	39.856	40	3 0 3	2.18	41.385	20	0 0 8
2.56742	34.9484	0	2.21	40.798	40	3 1 2	2.14	42.195	5	2 1 6
2.51501	35.701	0	2.18	41.385	20	2 1 7	2.08	43.473	30	3 0 4
2.31806	38.8507	0	2.08	43.473	60	3 1 4	1.993	45.474	40	3 1 4
2.2609	39.874	0	1.924	47.202	60	1 1 10	1.925	47.176	10	3 2 2
2.20136	40.9648	1	1.794	50.856	50	4 0 0	1.857	49.015	5	2 0 8
2.17761	41.4319	8	1.765	51.753	5	4 0 2	1.833	49.699	5	3 0 6
2.1765	41.5619	5	1.735	52.716	5	4 1 1	1.796	50.795	30	2 1 8
2.08189	43.4313	11	1.708	53.615	10	3 1 8	1.776	51.409	30	3 1 6
2.08174	43.5478	5	1.69	54.233	10	4 1 3	1.742	52.488	5	0 0 10
1.99829	45.3471	1	1.661	55.26	5	3 0 9	1.643	55.918	30	3 3 2
1.92617	47.1454	1	1.64	56.029	40	1 1 12	1.602	57.48	20	3 0 8
1.85711	49.0114	0	1.602	57.48	40	4 2 1	1.586	58.115	20	4 2 0
1.79133	50.937	0	1.584	58.195	10	4 2 2	1.561	59.137	60	4 2 2
1.74286	52.4597	1	1.562	59.096	20	1 0 13	1.422	65.599	20	1 0 12
1.73512	52.7117	1	1.532	60.372	50	3 1 10	1.395	67.034	5	1 1 12
1.64176	55.9634	1	1.427	65.341	30	1 1 14	1.377	68.029	30	3 1 10
1.60295	57.4429	0	1.378	67.973	40	3 1 12	1.352	69.465	10	4 1 8
1.56304	59.0523	0	1.362	68.883	30	1 0 15	1.325	71.092	10	5 1 4
1.53298	60.329	0	1.355	69.29	30	5 0 5	1.284	73.729	5	4 2 8
1.48757	62.3729	1	1.312	71.906	20	3 3 10	1.26	75.374	5	5 2 4
1.42421	65.4847	0	1.289	73.396	5	5 2 4	1.241	76.736	5	4 4 2
1.39459	67.0566	0	1.272	74.541	30	5 1 7	1.224	78.001	10	4 1 10
1.36339	68.8029	1	1.245	76.445	40	5 2 6	1.208	79.236	5	1 1 14
1.35969	69.0167	0	1.221	78.23	5	2 0 16	1.175	81.926	30	2 0 14
1.22465	77.9521	0	1.21	79.079	10	3 3 12	1.16	83.219	20	6 0 3
1.1581	83.386	0	1.201	79.79	5	5 1 9	1.127	86.235	10	6 1 4
			1.188	80.842	5	6 0 2	1.113	87.592	10	6 2 2
			1.178	81.673	5	4 1 13	1.101	88.796	5	3 0 14
			1.165	82.783	40	5 1 10	1.09	89.934	30	5 2 9
			1.146	84.469	20	4 0 14	1.077	91.324	10	1 0 16
			1.133	85.668	20	4 2 13	1.065	92.653	10	1 1 16
			1.127	86.235	20	3 1 16	1.051	94.264	10	5 2 10
			1.117	87.199	5	6 1 6	1.039	95.699	10	6 0 8
			1.092	89.724	50	5 1 12	1.029	96.937	20	6 1 8
			1.083	90.676	50	4 4 10	1.016	98.606	10	4 3 12
			1.059	93.335	40	5 3 10	1.006	99.94	10	5 1 12
			1.043	95.215	20	3 2 17	0.999	100.9	20	2 2 16
			1.036	96.066	40	2 1 19				
			1.022	97.827	40	5 1 14				
			1.013	99.002	5	7 1 1				
			1.004	100.212	20	5 3 12				
			1.001	100.623	30	6 1 11				
			0.998	101.039	30	2 0 20				
			0.995	101.46	40	3 0 19				
			0.991	102.027	10	6 4 2				

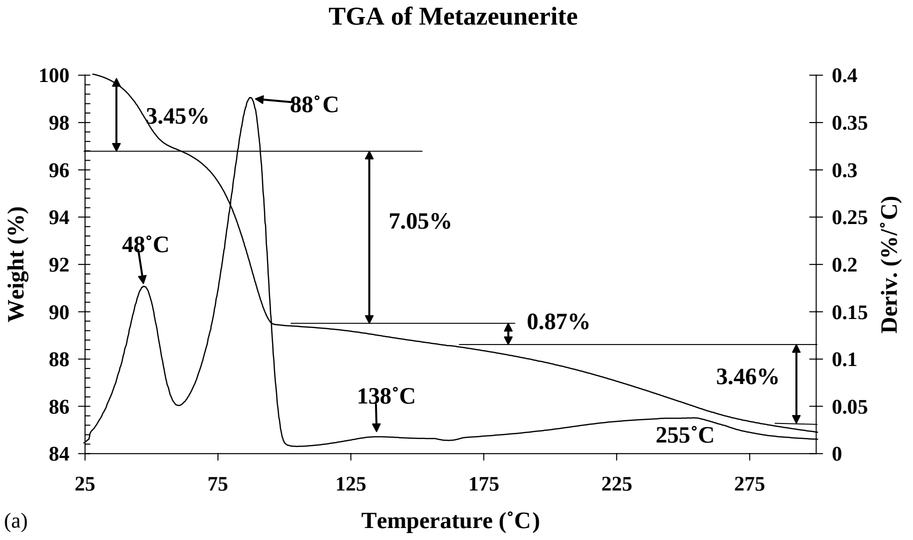

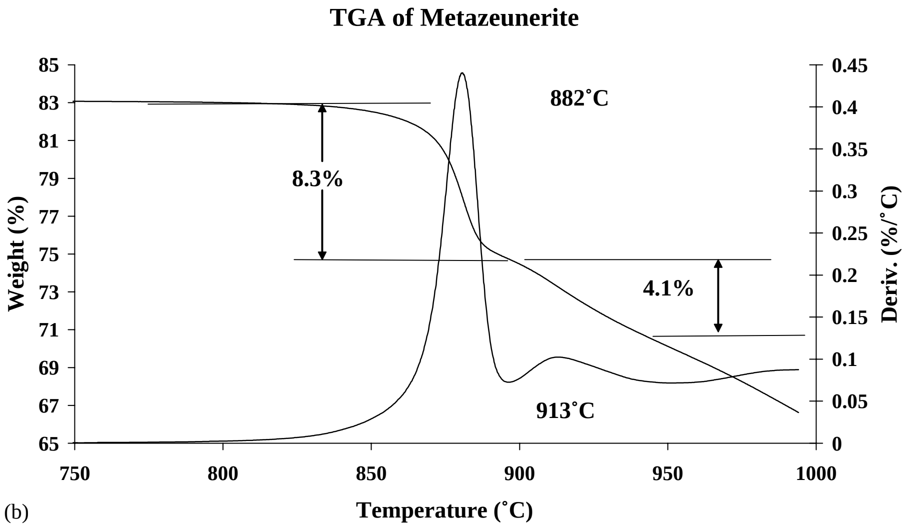

Fig. 1. High-resolution thermogravimetric analysis of metazeunerite.

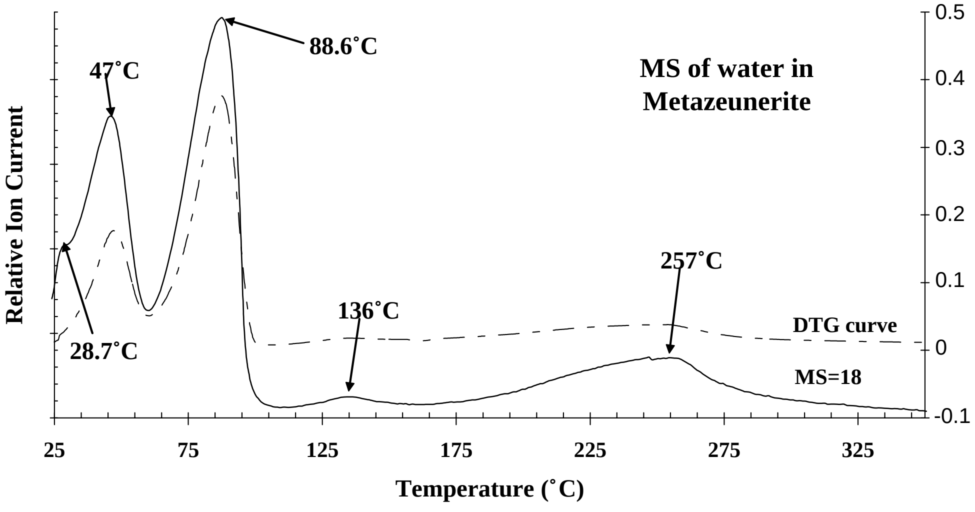

Fig. 2. DTG and MS of metazeunerite.

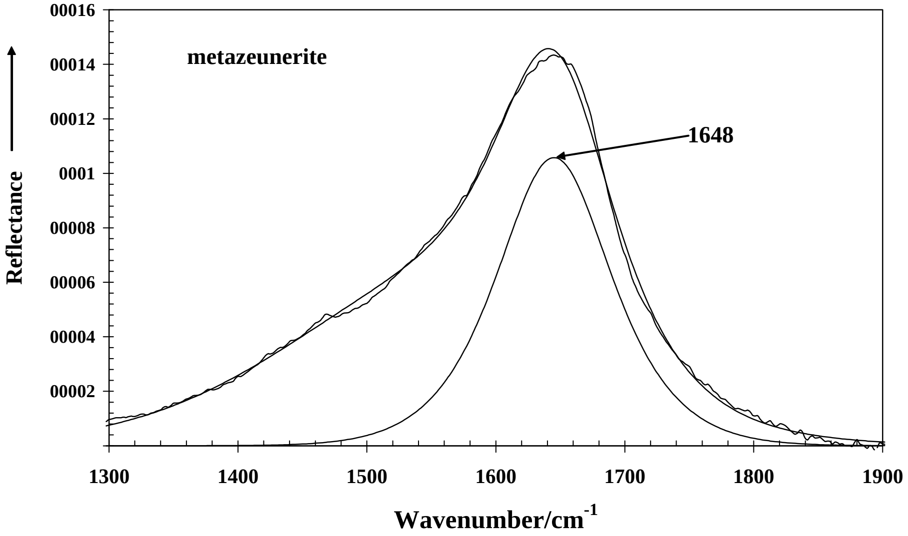

Fig. 3. Infrared spectrum of HOH bending region of the water.

loss does not match the theoretical weight loss. It may be possible that the As_2O_5 is condensing in the capillary before reaching the mass spectrometer.

Burns has shown that the U^{6+} cation is almost always present in crystal structures as part of a nearly linear $(UO_2)^{2+}$ uranyl ion that is coordinated by four, five or six equatorial anions in an approximate planar arrangement perpendicular to the uranyl ion, giving square, pentagonal and hexagonal bipyramids [26]. The crystal structure of metazeunerite has been undertaken [27]. Hanic [27] reported that the sheets $[(UO_2)(AsO_4)]$ are separated by layers containing the cations $(Cu(H_2O)_4)^{2+}$ and several moles of H_2O. However, this structure presented by Hanic is clearly incorrect [16]. The infrared spectrum of the hydroxyl stretching region of water of metazeunerite shows two intense bands at 3280 and 2923 cm^{-1} with a band of much lower intensity at 3407 cm^{-1}. Bands in these positions are indicative of strongly hydrogen bonded water. One possible model is based upon the water molecules coordinating the copper cation and at the same time hydrogen bonding to the AsO_4 units. The infrared spectrum of the HOH bending region of water in metazeunerite is shown in Fig. 3. Only a single HOH deformation band is observed at 1648 cm^{-1}. The reason for the tail on the lower wavenumber side of the spectrum may be attributed to δMOH bands [4]. The observation of a band in this position is an indication that no free water is present [28]. All of the water is in a structured state either in the interlayer or in the hydration sphere of the copper(II) cation.

3.3. Hot-stage Raman spectroscopy of metazeunerite

3.3.1. Raman spectroscopy of the hydroxyl stretching region using the thermal stage

The Raman spectra of the water OH stretching region of metazeunerite for selected temperatures are shown in Fig. 4. It should be noted that the intensity of the hydroxyl stretching region of metazeunerite is low and the hydroxyl stretching region occurs on a steeply sloping background making the determination of the spectra difficult. In the spectrum at 40 °C, four hydroxyl stretching bands are observed at 3748, 3537, 3394 and 3093 cm^{-1}. The bandwidths are 218, 97, 359 and 268 cm^{-1}. In the structure of metazeunerite, there are two symmetrically indepen-

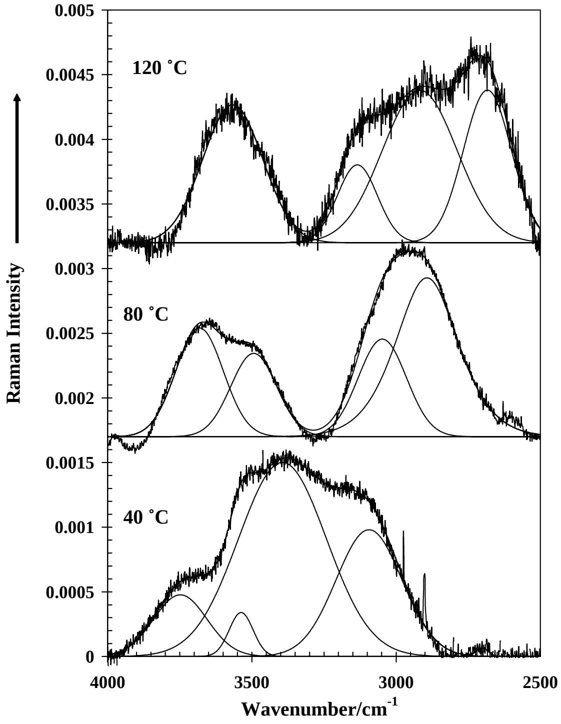

Fig. 4. Raman spectra of the hydroxyl stretching region of metazeunerite at 40, 80 and 120 °C.

dent water positions at room temperature leading to four water groups around the Cu^{2+} and four interstitial water groups. The observation of four OH stretching vibrations suggests that there are four independent water molecules in the metazeunerite structure. Locock and Burns [16] pointed out that in the crystal structure there are two free independent water molecules. The high wavenumber band at 3748 cm^{-1} may be ascribed to this weakly hydrogen bonded water molecule. Hydrogen bonds link these water molecules into the square planar sets of water molecules. The water molecules which coordinate the Cu^{2+} account for the bands observed at 3537, 3394 and 3093 cm^{-1}. In the first stage of thermal decomposition, two water molecules are lost at 48 °C. The Raman spectrum at 60 °C shows three OH stretching vibrations at 3436, 2953 and 2811 cm^{-1}. The position of these OH stretching vibrations suggests that partial dehydration in the first stage caused stronger hydrogen bonding in the metazeunerite structure. Further heating above 80 °C results in the loss of four molecules of water per formula unit. In the Raman spectrum of metazeunerite at 100 °C, four bands are observed at 3681, 3493, 3047 and 2893 cm^{-1}.

Raman spectroscopy shows changes in the structure of metazeunerite upon thermal treatment. The results from Raman spectroscopy support the concept that water is coming off in stages. Previous studies have suggested that the water is lost in a zeolite dehydration behaviour [29]. In such a situation, the water escapes through holes in a coherent three-dimensional framework. Such a process is reversible such that upon cooling the water would refill the spaces in the zeolite-type structure. The variable hydration state of zeolite-type materials is not consistent with the dehydration behaviour of metazeunerite. In contrast to porous materials, the water molecules are required to maintain the structural integrity. In this work, both the HRTG and the hot-stage Raman spectroscopy shows that the dehydration takes place as a series of steps. The question of reversibility of these hydration steps remains to be proven. The transition of zeunerite to metazeunerite may not be reversible. The reaction is as follows:

$$\begin{aligned}&Cu(UO_2)_2(AsO_4)_2 \cdot 12H_2O\\&\quad \rightarrow Cu(UO_2)_2(AsO_4)_2 \cdot 8H_2O + 4H_2O\end{aligned}$$

Such a reaction involves the removal of one layer of water either above or below the Cu^{2+} layer. Such a reaction involves the sideways displacement of this Cu^{2+} layer relative to the uranyl arsenate layer. Such displacement is likely to mean that the zeunerite to metazeunerite transition is non-reversible. Other researchers have investigated the dehydration behaviour of autunites, meta-autunite and other uranyl micas and found that the water content in existing phases is constant and does not vary as with zeolites [30,31]. Dehydration was found to proceed in a stepwise fashion [30,31]. Such structural arguments agree with the propositions propounded in this study.

3.4. Raman spectroscopy of the UO_2 and AsO_4 stretching region using the thermal stage

Cejka et al. [6,8,28,32] have reported the infrared spectroscopy of many uranyl minerals. The free uranyl ion $(UO_2)^{2+}$ with point symmetry D_{8h} should exhibit three fundamental modes symmetric stretching vibration ν_1, bending vibration ν_2 and the antisymmetric stretching vibration ν_3. The bending mode is doubly degenerate since it can occur in two mutually independent planes [28]. Hence, the linear uranyl group has four normal vibrations but only three fundamentals. In a linear symmetric uranyl ion belonging to the D_{8h} point group, the ν_1 band is found in the 900–750 cm^{-1} region and is Raman active but only appears in the infrared spectrum in the case of substantial symmetry lowering. The antisymmetric stretching vibration is active in the infrared and inactive in the Raman. Lowering of the symmetry results in the activation of all fundamentals. Farmer [33] reported the infrared spectral results of some autunite minerals. The values for torbernite were listed as ν_1 mode at 915 cm^{-1}, ν_2 as 465 cm^{-1}, ν_3 as 1115 and 1023 cm^{-1} and ν_4 as 615 and 550 cm^{-1}. Farmer gave the position of the $(UO_2)^{2+}$ bands as ν_1 at 805 cm^{-1} for torbernite and ν_3 as 915 cm^{-1}. The interpretation of this assignment is open to question. Cejka et al. [6] reported the infrared spectrum of sabugalite and suggested that the weak absorption band at 810 cm^{-1} was attributable to the symmetric stretching mode of the $(UO_2)^{2+}$ unit and that the band at 915 cm^{-1} was attributable to the antisymmetric stretching vibration of the $(UO_2)^{2+}$ unit. The ν_2 bands of the $(UO_2)^{2+}$ units were found at 298 and 254 cm^{-1}. Herein, lies the difficulty that both the ν_1 bands of AsO_4 and $(UO_2)^{2+}$ are found at the same spectral positions making interpretation by vibrational spectroscopy difficult.

The Raman spectra of the AsO_4 and UO_2 stretching region as a function of temperature are shown in Fig. 5. The results of the band component analyses are reported in Table 2. The symmetric stretching vibration of the aqueous arsenate anion (ν_1) is observed at 810 cm^{-1} and coincides with the asymmetric stretching mode (ν_3). The bending modes ν_2 and ν_4 are observed at 342 and 398 cm^{-1}, respectively. Herein, lies a problem in the vibrational spectroscopy of the arsenate containing uranyl micas. The bands associated with the AsO_4 stretching vibrations are coincident with the UO_2 stretching vibrations. A band is observed at 890 cm^{-1} and is sharp with a bandwidth of 10.0 cm^{-1}. This band is assigned in accordance with the attribution of Cejka et al. to the UO_2 ν_3 antisymmetric stretching modes. The band is asymmetric on the high wavenumber side suggesting two overlapping bands. Such a concept fits well with the non-equivalence of the two UO_2 bonds [16]. The band at 890 cm^{-1} shifts to 902 cm^{-1} upon thermal treatment above 50 °C. It is apparent that the loss of two water molecules according to stage 1 in the HRTG results changes the position of the ν_3 antisymmetric stretching vibration. These two water molecules are the two interstitial water molecules in the metazeuner-

Table 2
Raman spectroscopic analysis of metazeunerite at elevated temperatures

	20 °C	40 °C	60 °C	80 °C	100 °C	120 °C	Suggested assignments
Band centre (cm^{-1})	890	890	902	902	902	902	UO_2 ν_3 antisymmetric stretching
Bandwidth (cm^{-1})	10.0	16.0	18.2	30.9	17.4	19.2	
Relative intensity (%)	6.6	6.83	6.6	9.9	4.3	4.9	
Band centre (cm^{-1})			873	873	867		
Bandwidth (cm^{-1})			26.2	11.0	16.3		
Relative intensity (%)			4.0	0.5	0.87		
Band centre (cm^{-1})					844	842	UO_2 ν_1 stretching modes
Bandwidth (cm^{-1})					19.1	17.0	
Relative intensity (%)					8.8	8.0	
Band centre (cm^{-1})	818	822	813	822	813	810	UO_2 ν_1 stretching modes
Bandwidth (cm^{-1})	7.5	9.8	28.6	46.8	36.5	39.0	
Relative intensity (%)	45.8	21.5	32.0	32.0	30.4	37.1	
Band centre (cm^{-1})	811	811	801	807	804	805	UO_2 ν_1 stretching modes
Bandwidth (cm^{-1})	10.8	10.8	24.9	24.9	24.1	20.6	
Relative intensity (%)	47.6	70.5	36.8	28.4	24.1	17.9	
Band centre (cm^{-1})			775	777	776	778	Water librational modes
Bandwidth (cm^{-1})			30.5	34.5	34.3	24.0	
Relative intensity (%)			20.2	23.2	26.2	3.4	
Band centre (cm^{-1})	463	461					ν_4 bending modes of AsO_4
Bandwidth (cm^{-1})	19.0	62.7					
Relative intensity (%)	15.6	23.5					
Band centre (cm^{-1})	446	448	452	452	452		ν_4 bending modes of AsO_4
Bandwidth (cm^{-1})	20.1	17.4	37.3	37.3	37.3		
Relative intensity (%)	26.4	23.2	25.5	25.5	25.5		
Band centre (cm^{-1})	396	398					ν_4 bending modes of AsO_4
Bandwidth (cm^{-1})	10.8	18.8					
Relative intensity (%)	0.67	2.0					
Band centre (cm^{-1})	380		376	376	376		ν_2 bending modes of AsO_4
Bandwidth (cm^{-1})	12.8		49.7	49.7	49.7		
Relative intensity (%)	1.18		8.0	8.0	8.0		
Band centre (cm^{-1})	320	318	322	322	322		ν_2 bending modes of AsO_4
Bandwidth (cm^{-1})	7.1	6.6	16.7	16.7	16.7		
Relative intensity (%)	29.0	22.6	14.8	14.8	14.8		
Band centre (cm^{-1})	275	274	274	274	274		ν_2 bending modes of the $(UO_2)^{2+}$
Bandwidth (cm^{-1})	11.0	12.8	43.6	43.6	43.6		
Relative intensity (%)	0.87	2.0	10.1	10.1	10.1		
Band centre (cm^{-1})	235	241					ν_2 bending modes of the $(UO_2)^{2+}$
Bandwidth (cm^{-1})	18.9	15.7					
Relative intensity (%)	13.7	1.0					
Band centre (cm^{-1})	218	214	197	197	197		Cu–O_{uranyl} stretch (?)
Bandwidth (cm^{-1})	15.0	14.6	28.7	28.7	28.7		
Relative intensity (%)	1.4	10.5	11.3	11.3	11.3		
Band centre (cm^{-1})		182	152	152	152		Lattice modes
Bandwidth (cm^{-1})		10.8	19.6	19.6	19.6		
Relative intensity (%)		13.6	13.3	13.3	13.3		
Band centre (cm^{-1})		139	137	137	137		Lattice modes
Bandwidth (cm^{-1})		14.7	11.6	11.6	11.6		
Relative intensity (%)		1.4	8.1	8.1	8.1		

ite structure. The bandwidth of the 890/902 cm^{-1} band increases and then decreases upon thermal treatment with the maximum bandwidth at 80 °C.

In the 20 °C spectrum, two bands are observed at 818 and 811 cm^{-1} with bandwidths of 7.5 and 10.8 cm^{-1}. The first band shifts to 822 cm^{-1} at 40 °C. However, there is a significant change in the relative intensities of the 818/811 cm^{-1} bands upon heating from 20 to 40 °C. These two bands are assigned in accordance with Cejka [28] as the ν_1 stretching modes of the UO_2 units. It is possible that the

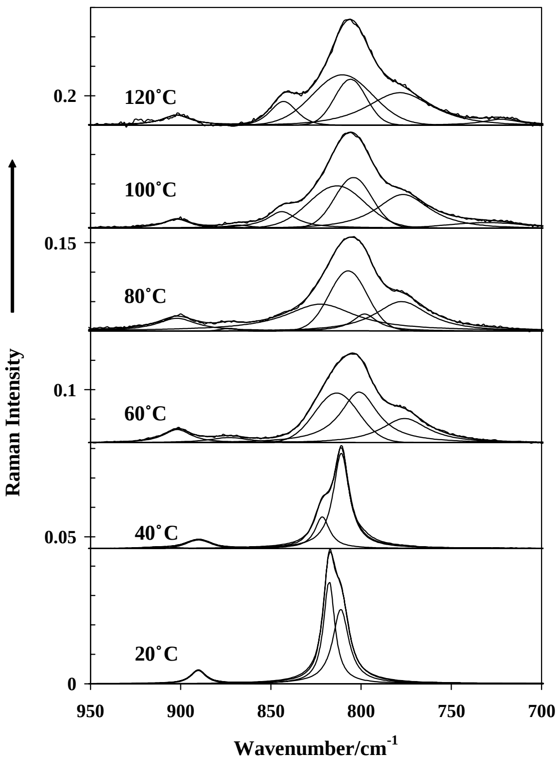

Fig. 5. Raman spectra of the UO_2 and AsO_4 stretching region of metazeunerite at 20, 40, 60, 80, 100 and 120 °C.

change in the band position of the 818 cm^{-1} band is due to an intensity contribution from the symmetric stretching mode of the AsO_4 units. Alternatively, the band is an additional band brought about through a stronger bonding of the UO_2 to the Cu^{2+} cations. Dehydration forces the Cu^{2+} to bond to the UO_2 groups. This bonding is observed as increased intensity in the ~854 and 841 cm^{-1} bands. This means that the two UO_2 bands at ~825 and 807 cm^{-1} are associated with non-bonding or weak bonding. In the structure of zeunerite proposed by Locock and Burns, the Cu^{2+} is bonded to two uranyl oxygens linearly at long interatomic distances of 2.482 Å. In the structure of metazeunerite, the $Cu–O_{uranyl}$ bond distances are 2.445 and 2.645 Å. Dehydration forces the distance between the UO_2 units and the Cu^{2+} to increase slightly. The reason for this slight increase is the shuffling of the uranyl arsenate layer relative to the Cu^{2+} atoms. This results in the additional band in the UO_2 stretching region.

Upon heating the metazeunerite to 60 °C, the band profile broadens and becomes more complex. The two bands now shift to 813 and 801 cm^{-1} and are attributed to the UO_2 symmetric stretching vibrations. At the same time, an additional band at 873 cm^{-1} is observed. This band is assigned to the ν_3 antisymmetric stretching mode of the AsO_4 units. The non-equivalence of the two UO_2 bonds affects the AsO distances and results in the non-equivalence of the AsO_4 bonds. In terms of Raman spectroscopy, this means that the AsO_4 symmetric stretching vibration will be either inactive or of low intensity. Alternatively, the UO_2 and AsO_4 symmetric stretching vibrations couple and only one band is observed. Thermal treatment above 80 °C results in the appearance of an additional band at 844 cm^{-1}, which is assigned to the ν_1 AsO_4 symmetric stretching vibration. The effect of thermal treatment with dehydration results in the uncoupling of the UO_2 and AsO_4 symmetric stretching vibrations. In the 80 °C spectrum, the two UO_2 stretching vibrations are observed at 822 and 807 cm^{-1} and are broad with bandwidths of 46.8 and 24.9 cm^{-1}. Significant changes are observed in the band profile in the 750–850 cm^{-1} region upon heating from 80 to 100 °C. These changes are associated with the loss of water in stage 2 of the dehydration steps at 88 °C. The Raman spectra above 50 °C show an additional band at around 775 cm^{-1}. This band is assigned to a water librational mode. The band becomes Raman active after 60 °C and probably results from the hydrogen bonding of water to the AsO_4 units. It is noted that the intensity approaches zero in the 120 °C spectrum.

3.5. Raman spectroscopy of the AsO_4 bending region using the thermal stage

The Raman spectroscopy of the UO_2 and AsO_4 bending region has the advantage that the two bending regions are well separated (Fig. 6). The AsO_4 bending region occurs between 300 and 500 cm^{-1} and the UO_2 bending region below 300 cm^{-1}. The bending modes (ν_2) of aqueous AsO_4 occur at 342 cm^{-1}. Thus, the sharp band at 320 cm^{-1} for metazeunerite is assigned to the OAsO in plane bending mode. The

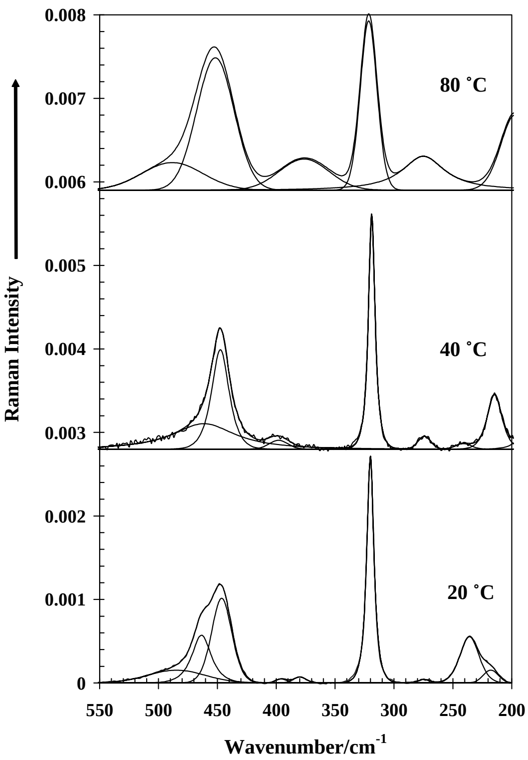

Fig. 6. Raman spectra of the AsO_4 bending region of metazeunerite at 40, 80 and 120 °C.

band at 20 and 40 °C is sharp with bandwidths of 7.1 and 6.6 cm^{-1}, respectively. At 60 °C, the band is observed at 322 cm^{-1} with an increased bandwidth of 16.7 cm^{-1}. The bending mode (ν_4) of the AsO_4 is observed at 398 cm^{-1} in aqueous systems. In the 20 °C spectrum, four bands are observed at 463, 446, 396 and 380 cm^{-1}. The latter two bands are of low intensity. All four bands are quite sharp with bandwidths of 19.0, 20.1, 10.8 and 12.8 cm^{-1}, respectively. At 40 °C, three bands are observed at 461, 448 and 398 cm^{-1} with considerably increased bandwidths. At 60 °C and above, only a single band is observed at 452 cm^{-1}. The significance of the changes in the spectrum of the ν_4 bending region is the removal of the loss of degeneracy upon thermal treatment. An additional broad band is observed at 376 cm^{-1} and is assigned to a second ν_4 bending mode.

In the very low wavenumber region, three bands are observed in the 298 K spectrum at 275, 235 and 218 cm^{-1}. The bands at 275 and 235 cm^{-1} are attributed to the ν_2 bending modes of the $(UO_2)^{2+}$ units. The band at 218 cm^{-1} is assigned to lattice vibrations. Other bands are observed around 182 and 139 cm^{-1} and are also described as lattice modes.

4. Conclusions

A combination of high-resolution thermogravimetric analysis coupled to a gas evolution mass spectrometry has been used to study the thermal decomposition of the mineral metazeunerite ($Cu(UO_2)_2(AsO_4)_2{\cdot}8H_2O$). Five stages of weight loss are observed at 48, 88, 125, 882 and 913 °C. In the first three stages 2, 4 and 2 mol of water are lost. In stages 4 and 5, As_2O_5 units are lost and it is probable that reduction of the As, U and even Cu occurs. The stages of dehydration were confirmed by the use of evolved water vapour mass spectrum. The temperatures of these dehydration steps were then used as the temperatures at which Raman spectra of the thermally decomposed sample were obtained. These Raman spectra were then used to characterise the changes in the molecular structure of the metazeunerite. Very significant changes in the Raman spectra were obtained at these temperatures. The crystal structure of metazeunerite shows that the structure is a tetragonal structure. This distortion is maintained by the hydrogen bonding of the water molecules to the AsO_4 and UO_2 units which form a layer either above or below the plane of the Cu^{2+} atoms. The loss of water between 40 and 55 °C results in the removal of interstitial water resulting in Raman spectra of increasing complexity. Further dehydration above 100 °C results in the loss of the layer structure, resulting in further increased complexity in the Raman spectra. Dehydration of the mineral is readily followed by the changes in the spectra of the water OH stretching region.

One of the difficulties in assigning the bands of the autunite–meta-autunite minerals is the overlap of the stretching vibrations of the UO_2 and AsO_4 and/or PO_4 units. The AsO_4 and UO_2 stretching vibrations occur in almost identical positions. The further complexity is introduced because of the distorted structure of the metazeunerite unit cell. In the structure of metazeunerite the four AsO bonds are non-equivalent brought about by the non-equivalence of the two UO_2 bonds. Such non-equivalence results in the lack of intensity of the ν_1 AsO_4 stretching band. This band only becomes observed after the initial dehydration steps which results in the removal of the layered water structure. No symmetric stretching vibration is observed until after significant dehydration has occurred at 80 °C, when a low intensity band at 827 cm^{-1} is observed. The structure of metazeunerite is such that the two UO bonds are non-equivalent. These results in the observation of two UO stretching bands observed at 818 and 811 cm^{-1}. A low intensity band is observed at around 890 cm^{-1} and is attributed to the UO_2 antisymmetric stretching vibration. A complex set of bands is observed in the low wavenumber region. These bands are assigned to the UO_2 bending vibrations. Bands are observed at 275, 235, 218 and 182 cm^{-1} and are all assigned to UO_2 bending modes. The complexity of the UO_2 bending modes is observed up to 250 °C. This complexity is lost only after dehydration.

References

[1] I.M. Threadgold, CSIRO Mineragraphic Investigations Technical Paper No. 2, 1960.
[2] R.L. Frost, T. Kloprogge, M.L. Weier, W.N. Martens, Z. Ding, H.G.H. Edwards, Spectrochim. Acta A Mol. Biomol. Spectrosc. 59 (2003) 2241.
[3] R.L. Frost, M.L. Weier, W. Martens, J.T. Kloprogge, Z. Ding, Thermochim. Acta 403 (2003) 237.
[4] P. Burns, Rev. Mineral. 38 (1999) 23.
[5] H. Isobe, R.C. Ewing, T. Murakami, Mater. Res. Soc. Symp. Proc. 333 (1994) 653.
[6] J. Cejka, Z. Urbanec, J. Cejka Jr., J. Ederova, A. Muck, J. Therm. Anal. 33 (1988) 395.
[7] T.L. Ambartsumyan, Atomnaya Energ., Voprosy Geol. Urana, Suppl. 6 (1957) 86.
[8] J. Cejka, J. Cejka Jr., A. Muck, Thermochim. Acta 86 (1985) 387.
[9] T. Muto, Mineral. J. 4 (1965) 245.
[10] A.J. Locock, P.C. Burns, Am. Mineral. 88 (2003) 240.
[11] J. Cejka Jr., A. Muck, J. Cejka, Phys. Chem. Miner. 11 (1984) 172.
[12] C. Frondel, Am. Mineral. 36 (1951) 680.
[13] S.A. Miller, J.C. Taylor, Z. Kristallogr. 177 (1986) 247.
[14] J. Beintema, Recueil des Travaux Chimiques des Pays-Bas et de la Belgique 57 (1938) 155.
[15] P.C. Burns, M.L. Miller, R.C. Ewing, Can. Mineral. 34 (1996) 845.
[16] A.J. Locock, P.C. Burns, Can. Mineral. 41 (2003) 489.
[17] K. Walenta, Chemie der Erde 24 (1965) 254.
[18] W. Martens, R.L. Frost, P.A. Williams, J. Raman Spectrosc. 34 (2003) 104.
[19] W.N. Martens, R.L. Frost, J.T. Kloprogge, P.A. Williams, Am. Mineral. 88 (2003) 501.
[20] R.L. Frost, M.L. Weier, Thermochim. Acta 406 (2003) 221.
[21] R.L. Frost, Z. Ding, Thermochim. Acta 405 (2003) 207.
[22] E. Horvath, R.L. Frost, E. Mako, J. Kristof, T. Cseh, Thermochim. Acta 404 (2003) 227.
[23] R.L. Frost, M. Crane, P.A. Williams, J.T. Kloprogge, J. Raman Spectrosc. 34 (2003) 214.
[24] R.L. Frost, Spectrochim. Acta A Mol. Biomol. Spectrosc. 59A (2003) 1195.

[25] W. Martens, R.L. Frost, J.T. Kloprogge, J. Raman Spectrosc. 34 (2003) 90.
[26] P.C. Burns, R.C. Ewing, F.C. Hawthorne, Can. Mineral. 35 (1997) 1551.
[27] F. Hanic, Czechoslovak J. Phys. 10 (1960) 169.
[28] J. Cejka, Rev. Mineral. 38 (1999) 521.
[29] C. Frondel, Am. Mineral. 36 (1951) 680.
[30] K. Walenta, Jahresh. Geol. Landesamtes Baden-Wuerttemberg 6 (1963) 113.
[31] R. Vochten, A. Goeminne, Phys. Chem. Miner. 11 (1984) 95.
[32] J. Cejka Jr., A. Muck, J. Cejka, Neues Jahrbuch fuer Mineralogie, Monatshefte 3 (1985) 115.
[33] V.C. Farmer, Mineralogical Society Monograph 4: The Infrared Spectra of Minerals, 1974.